ARMY RESEARCH LABORATORY

A Multidisciplinary Coupled Computational Fluid Dynamics (CFD) and Structural Dynamics (SD) Analysis of a 2.75-in Rocket Launcher

Karen R. Heavy, Jubaraj Sahu,
and Stephen A. Wilkerson

ARL-MR-529 April 2002

The findings in this report are not to be construed as an official Department of the Army position unless so designated by other authorized documents.

Citation of manufacturer's or trade names does not constitute an official endorsement or approval of the use thereof.

Destroy this report when it is no longer needed. Do not return it to the originator.

Army Research Laboratory
Aberdeen Proving Ground, MD 21005-5066

ARL-MR-529 April 2002

A Multidisciplinary Coupled Computational Fluid Dynamics (CFD) and Structural Dynamics (SD) Analysis of a 2.75-in Rocket Launcher

Karen R. Heavey, Jubaraj Sahu, and
Stephen A. Wilkerson
Weapons and Materials Research Directorate, ARL

Abstract

A multidisciplinary effort was undertaken to investigate the effect of aerodynamic loading on the structural integrity of a multiple launch rocket system of interest to the U.S. Army. Computational fluid dynamics (CFD) techniques have been used to obtain numerical solutions for the flow field of a rocket and launcher. Computed results have been obtained for several launch tubes, with the rocket at separation distances of 20, 33, and 66 in. Qualitative flow field features show the surface pressure on the surface of both the projectile and the launcher. The surface pressure data on the launcher was then extracted from the solution files. Software was developed to couple this data to a structural dynamics (SD) solver. CFD results provided the aerodynamic loading component used during the initial portion of the launch sequence. The SD code was subsequently used to calculate stress points on the launcher. These results represent a first step in an effort to generalize and fine tune the CFD/SD interface.

Acknowledgments

This work was supported by a grant of computer time from the Department of Defense High Performance Computing Major Shared Resource Center at the U.S. Army Research Laboratory.

INTENTIONALLY LEFT BLANK.

Contents

INTENTIONALLY LEFT BLANK.

List of Figures

1. Introduction

The advancement of computational fluid dynamics (CFD) is beginning to have a major impact on projectile design and development [1–4]. Improved computer technology and state-of-the-art numerical procedures enable scientists to develop solutions to complex three-dimensional (3-D) problems associated with projectile and missile aerodynamics. The research effort has focused on the development and application of a versatile overset grid numerical technique to solve geometrically complex singlebody and multibody aerodynamic problems. This numerical capability has been used successfully to determine the aerodynamics on a number of projectile configurations [4–6] at transonic and supersonic speeds. Earlier applications involved axisymmetric flow computations [4, 5]. Recently, this technique has been used to investigate submunition dispersal from an Army tactical missile system [6] involving 3-D flow computations.

This report describes the application of the advanced numerical technique to a multiple launch rocket system (MLRS) of interest to the U.S. Army. Figure 1 shows a photograph of an MLRS mounted on a helicopter. The focus of this study is on the rocket body and the launcher pod. The computational problem involves 3-D flow computations of rockets being released from multiple tubes located in the launcher pod. The scope of this study is limited to a single rocket launched from a selected tube. Figure 2 shows the computational model of the launcher with a rocket being released from the center tube. The particular problem here is to determine the resulting surface pressure on the launcher when the rocket is released from various launch tubes, to include the center tube and two other asymmetric tube locations (Figure 3). The pressure data on the surface of the pod is extracted and used with a structural dynamics (SD) code to help identify the high-stress regions on the launcher.

The complexity and uniqueness of this type of problem result from the aerodynamic interference of the individual components, which include 3-D shock-shock interactions, shock-boundary layer interactions, and highly viscous-dominated separated wake flow regions. The overset grid technique [7–9], which is ideally suited to this problem, involves generating numerical grids about each body component and then oversetting them onto a base grid to form the complete model. With this composite overset grid approach, it is possible to determine the 3-D interacting flow field of the system and the associated aerodynamic forces and moments without the need for costly regridding. The solution procedure of the developed technique is to compute the interference flow field at multiple locations until final converged solutions are obtained and then to integrate the pressure and viscous forces to obtain the total forces and moments.

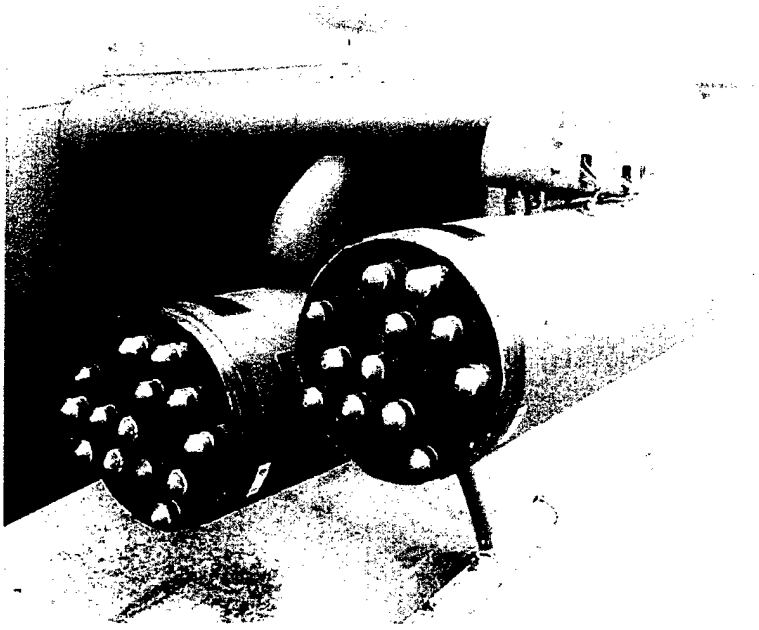

Figure 1. Photograph of an MLRS.

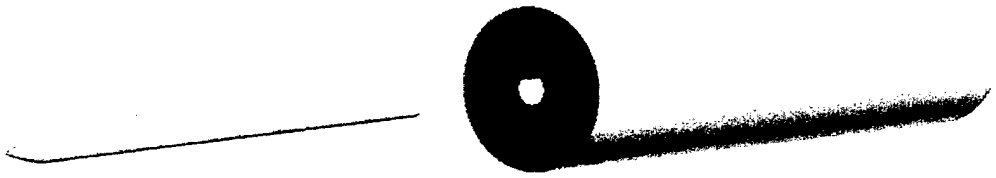

Figure 2. Computational model of a rocket with launcher.

A description of the numerical technique and the Chimera technique is provided. The coupling procedure between CFD and SD is described. The model geometry and the various computational grids used for the numerical computations are described in detail. Steady-state computational results are presented for various launch tube locations, as well as separation distance between the rocket and launcher. Finally, the surface pressure data extracted from the CFD results is interpolated and applied to the structural analysis of the rocket launcher.

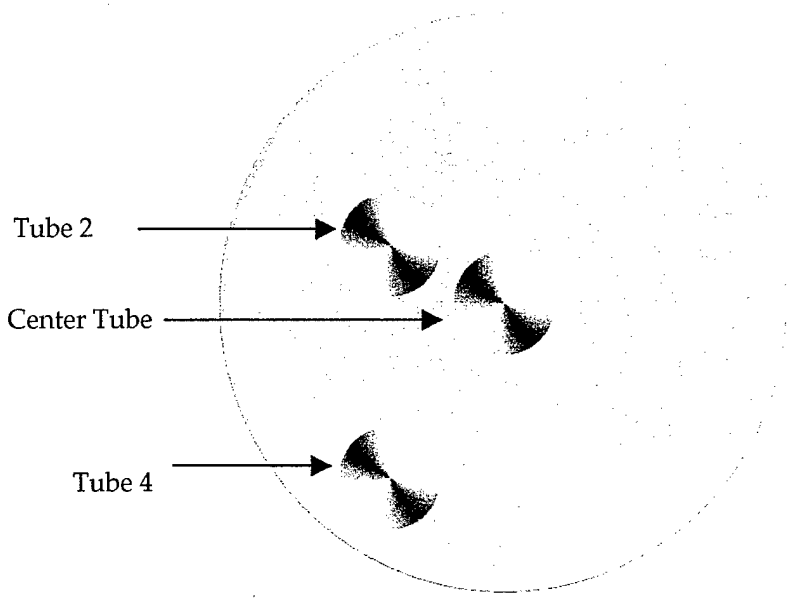

Figure 3. Computational model showing selected tube locations.

2. CFD Solution Technique

2.1 ZNSFLOW Solver

The ZNSFLOW solver is a product of a common high-performance computing software support initiative (CHSSI) project [10]. It is a descendant of F3D [11], a code used successfully for many years on Cray vector processors such as the C90. Under CHSSI, it was rewritten to provide scalable performance on a number of computer architectures. Programming enhancements include the use of dynamic memory allocation and highly optimized cache management. ZNSFLOW is highly portable and features a graphical user interface to facilitate problem setup. It has been used extensively in the computation of flow field calculations for projectile and missile programs of interest to the U.S. Army [1–4]. The flow solver includes the Chimera [7–9] overset discretization technique for CFD modeling of complex configurations. By using the Chimera technique, one can greatly simplify the grid topology and grid generation for very complex systems. One of the drawbacks in using the Chimera technique has been the increased complexity and corresponding confusion in applying a turbulence model. A Chimera model can be composed of multiple zones, with each zone possibly having a unique grid topology. Most turbulence models have specific direction-, orientation-, or distance-related requirements for correct application. For a complex Chimera model, applying a turbulence model can be a very complex process, especially an algebraic model such as the Baldwin-Lomax [12] model.

This problem has been addressed in ZNSFLOW by installing pointwise one- and two-equation turbulence models [13] that are not orientation specific. This greatly simplifies the setup of the turbulence model. Wall location information is supplied when the wall boundary conditions are set by the user.

2.2 Chimera Composite Grid Scheme

The Chimera overset grid scheme [7–9] is a domain decomposition approach where a configuration is meshed using a collection of overset grids. It allows each component of the configuration to be gridded separately and overset into a main grid. Overset grids are not required to be joined in any special way. Usually, there is a major grid that either covers the entire domain or is generated about a dominant body. Minor grids are then generated about the remainder of the bodies. Because each component grid is generated independently, portions of one grid may be found to lie within the solid surface boundary contained within another grid. Such points lie outside the computational domain and are excluded from the solution process.

In the rocket launcher study, there is a background grid that serves as the major grid. The grids around the rocket and launcher are considered minor grids. The minor grids are completely overlapped by the major grid; thus, each boundary can obtain information by interpolation from the major grid. Similar data transfer or communication is needed from the minor grids to the major grid. However, a natural outer boundary that overlaps these grids does not exist. The Chimera technique creates an artificial boundary (also known as a hole boundary) between grids to provide the required path for information transfer from the rocket and launcher grids to the background grid. The resulting hole region is excluded from the flow field solution in the rocket body grid. The set of grid points that form the border between the hole points and the normal field points are called intergrid boundary points. These points are updated by interpolating the solution from the overset grid that created the hole.

A major part of the Chimera overset grid approach is the information transfer from one grid to another by means of the intergrid boundary points. Again, these points consist of a set of points that define the hole boundaries and outer boundaries of the minor grids. These points depend on the solutions in the overlapping regions. In the present work, the PEGSUS code [14] has been used to establish the linkages between the various grids that are required by the flow solver or aerodynamics code described earlier. These include determining the interpolation coefficients and the setting up of Chimera logic for bodies making holes in overlapping grids.

2.3 Boundary Conditions

For simplicity, most of the boundary conditions have been explicitly imposed. For the background grid, free stream boundary conditions are used at the inflow boundary as well as at the outer boundary. The no-slip boundary condition is used on both the rocket and launcher surfaces; it has been modified, however, to include a jet flow from the rear of the rocket. The pressure at the wall is calculated by solving a combined momentum equation. A combination of symmetry and extrapolation boundary conditions is used at the centerline (axis) for all grids. For the two-dimensional (2-D) cases, a symmetry boundary condition is imposed at the circumferential edges of all grids. For the 3-D case, ZNSFLOW requires that circumferential boundary conditions be set; this is accomplished by adding an overlapping plane and copying the dependent variables from one plane to another. Boundary conditions are not applied at the outer boundaries of the rocket and launcher grids; instead, they are updated through the Chimera interpolation procedure.

3. SD Coupling

Coupling CFD solutions with SD calculations is needed for many Army design and evaluation applications. In the early 1980s, codes like EPIC, PIECES, and DYSMAS-ELC [15] made headway in coupling CFD Navier-Stokes calculations with SD calculations. However, many of the coupled calculations were related to shock loading and damage from UNDEX munitions and ignored the longer time dynamic response of the structure. Other efforts focused on closed-form laminar flow calculations coupled with axisymmetric structures using modal-superposition solutions while ignoring the shock loading [16]. Both methods had some value but with severe limitations. On the other hand, the method described here takes a step toward developing coupling constraints between CFD codes and SD codes in a general application.

The calculations presented here serve as a first step in creating a tool for Army applications where both CFD and SD results are required prior to design. In particular, the airflow loads from a departing 2.75-in rocket plume are calculated using the ZNSFLOW solver discussed previously. The calculated pressures are applied to the structural model and the response is observed. The end goal of this approach is to conduct independent CFD and structural calculations that are coupled in a time stepping scheme. In other words, the results from one of the codes would be the input to the other and vice versa. The resulting computation would be quite robust, but very tedious. Additionally, the code writing for the coupling of the codes would take a multi-year multi-man effort well beyond the scope of the current project. Hence, a step-by-step process in building this

capability is presented. In order to better understand the logic of this process, a brief overview of the approach is given.

Listed below are several of the major barriers that need to be solved in order to couple these two different numerical approaches:

- approximations in geometry,
- differences in gridding density,
- transfer of loading,
- time step differences,
- asymmetric and 3-D calculations, and
- cross talk between the codes.

3.1 Approximation Technique

Approximations in geometry are done by the analyst based on past experience and knowledge of the effects on the overall accuracy of the model. Sometimes this is accomplished in steps by gradually increasing the complexity of the model while examining the change in results to see the importance of including or excluding modeling details. For this project, geometry approximations were accomplished through discussions between the CFD and SD modelers. Attributes such as the protruding rockets (see Figure 1) or the lip on the front rocket pod needed to be agreed upon prior to building the CFD and finite element method (FEM) models. Additionally, determining which rocket tubes had rockets in them and which were empty was equally important. The first and most basic approach (see Figure 2) shows an axisymmetric configuration with the center rocket being fired. The follow-on to this first calculation included rockets from asymmetric positions (see Figure 3). For these calculations a simple cylinder was used with only the rocket being expelled having its tube open. Remember, this was a proof of principle calculation rather than an actual simulation of the firing order of the 2.75-in rocket pod. Equally important was the fact that the contribution to pod flexure caused by an open rocket tube was unknown. Increased complexity in the model was added only after the initial calculation was successfully performed. From a structural stand point, the rocket tubes and the rocket pod ribs add structural support and need to be included in the model. However, they hold no importance to the CFD calculation. Hence, only the surface used in the CFD calculations and SD calculations need to be in common. This presents some interesting problems in the automation of the process of coupling the two approaches.*

*Without automation, the load transfer process becomes time consuming and expensive. Additionally, the automation process must be well understood prior to models being built, or the resulting models will require numerous time intensive manual adjustments.

3.2 Grid Density

Differences in gridding density represent one of the more interesting problems faced by a researcher trying to couple these solution techniques. A robust algorithm is ultimately needed to take the loading from the CFD calculation and apply the loads to the surface of the model (Figure 4).

Figure 4. Differences in gridding locations and density between CFD and FEM grids.

The algorithm must take into account the differences in gridding and gaps caused by subtle differences in the models' geometry. Furthermore, the algorithm must interpolate or average the pressure profile along the surface of the FEM model. This becomes more complicated for 3-D problems. The algorithm must also know which surfaces to pressurize on the FEM model. This is no small task, as the thickness of a shell element may be of the same order as the gaps between the CFD and FEM grids. Therefore, care must be taken in assembling the FEM models outward pointing normal vectors.

3.3 Load Transfer

The transfer of loading was accomplished by having the CFD modelers provide pressure time histories with an xyz coordinate system from their computational results. This data was read into an algorithm that identified the external elements in the FEM model and then interpolated the CFD pressure field as an equivalent normal pressure. A stair-stepping pressure profile was used in this technique. In order to transfer the pressure load, a computer program was written using the Visual Basic programming language. The program calculated the outward normal of each element's face and then looked for the elements on the surface (Figure 5). These elements formed a basis for a comparison with the CFD calculations.

The CFD calculations provided a higher level of resolution than was necessary for the structural calculations. The loads were therefore averaged over the surface of the element, and an equivalent pressure was applied to the surface (Figure 6). The pressure profile was then applied over the surface of the rocket

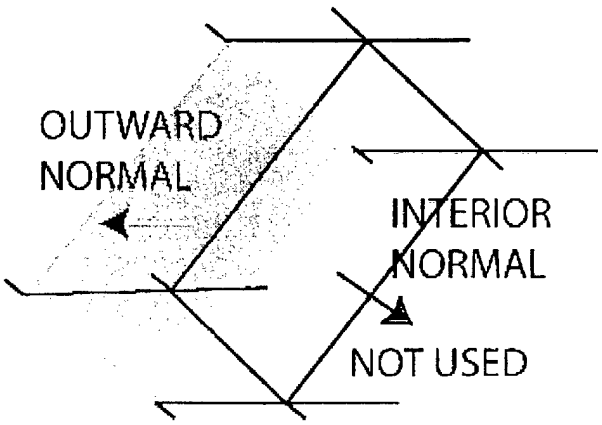

Figure 5. Outward surface normal needed from each element in the model.

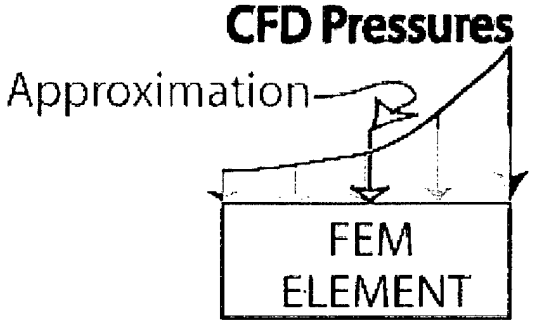

Figure 6. Pressure approximation used in current algorithm.

pod, and a steady-state structural analysis was performed. Although the CFD calculations were 3-D, this initial coupling effort used a 2-D pressure profile that was applied symmetrically over the FEM model used in the SD analysis. Time step differences, asymmetric and 3-D calculations, and cross talk between the codes were not addressed in the current effort.

4. Model Geometry and Computational Grid

4.1 CFD Model and Grid

The computational model consists of a 2.75-in rocket with launcher. The rocket is an ogive cylinder with a length of 66 in. The launcher is a cylinder of similar length containing 19 launch tubes, although only 3 are modeled in this case

(see Figure 3). The diameter of the launcher is 15.5 in. Additionally, the rocket is modeled at three different separation distances (S) from the launcher. Figure 7 shows these configurations for the center tube.

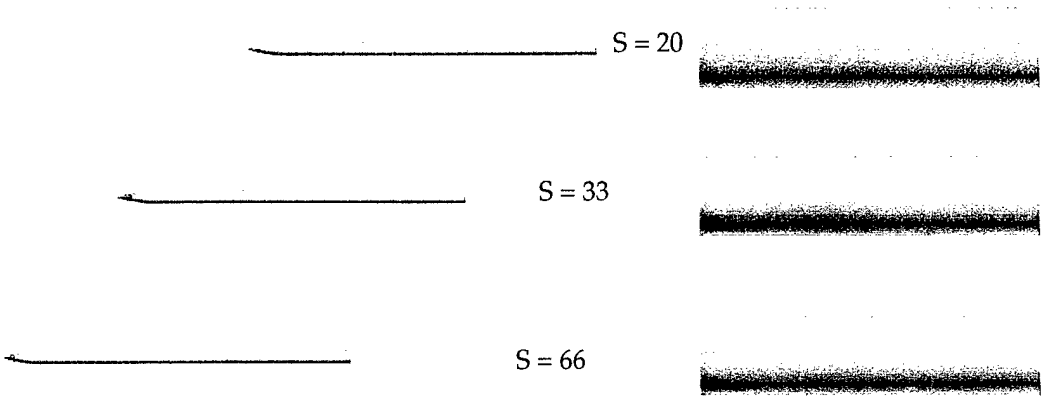

Figure 7. Computational model showing various separation distances.

The computational mesh for each of these configurations is quite complex. The entire grid system contains ~3.9-million grid points and consists of six sections. One large grid provides the background mesh for the entire flow field. A single smaller grid provides the mesh around the rocket. The computational mesh for the launcher, however, is more complex. Four grids are used to model the launcher: the launch pod itself, the launch tube (inside the pod), and a grid at each end of the tube. Each grid section was obtained separately and then overset to provide the full grid. The grid dimensions for the background grid are 290 × 62 × 70, in the longitudinal, circumferential, and radial directions, respectively, 155 × 92 × 64 for the rocket, 196 × 92 × 64 for the launcher, 102 × 92 × 64 for the tube, and 25 × 92 × 40 for the grid at each end of the tube. The final computational meshes were created using the various tools found in the OVERGRID grid generation software package [17]. Figure 8 shows a cross-sectional view of the longitudinal grid system for this complex configuration.

As stated earlier, the Chimera technique allows individual grids to be generated with any grid topology, thus making the grid generation process easier. For this study, the rocket was initially positioned along the longitudinal line of symmetry, simulating a launch from the center tube. A geometric translation was used to place it at separation distances of 20, 33, and 66 in (S = 20, S = 33, and S = 66, respectively) in front of the launcher (see Figure 7). Likewise, there was no need to regrid in order to generate the tube grids—a geometric translation was used to place the original (center tube) grid in the desired position. As part

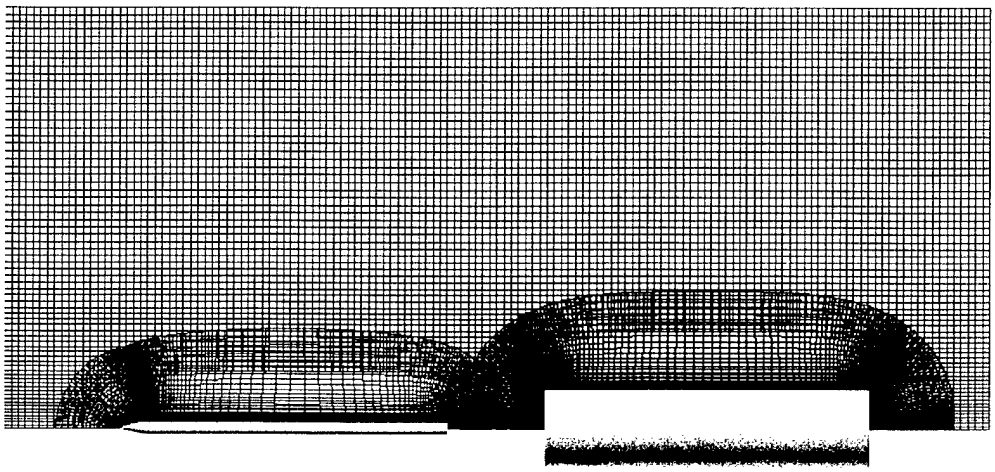

Figure 8. Longitudinal view of the computational mesh.

of the Chimera blanking procedure, the tube grid cuts a hole in the surface of the launcher pod grid. This same process was also used to reposition the rocket grids and recut the holes in the background grid. All grid points in the background grid that lie within the holes are blanked out and are excluded from the flow field solution process. Also, all points on the hole boundary in the background grid are updated through interpolation of the solution for the grids around the rocket and launcher. Figure 9 is an expanded view of the grid on the forward surface of the launcher, showing the results of the Chimera overlap and hole cutting process for the center tube. This hole-cutting procedure was done for all of the other cases as well.

4.2 FEM Model

The model of the rocket pod was constructed using the HYPERMESH pre- and postprocessor for the ANSYS solver. The model consists of four noded shell elements. Each rocket tube was represented with an individual tube. Additionally, both end plates were included and the two center ribs were also modeled. The skin around the attachment points was also made thicker to reflect the changes in thickness at that location. Initially, the attachment points were assumed semi-rigid (Figure 10).

Subsequent models included a crude mounting unit, as shown in Figure 11. The boundary constraints were formulated based on observations from an actual rocket pod. The rack was then supported rigidly at its attachment points.

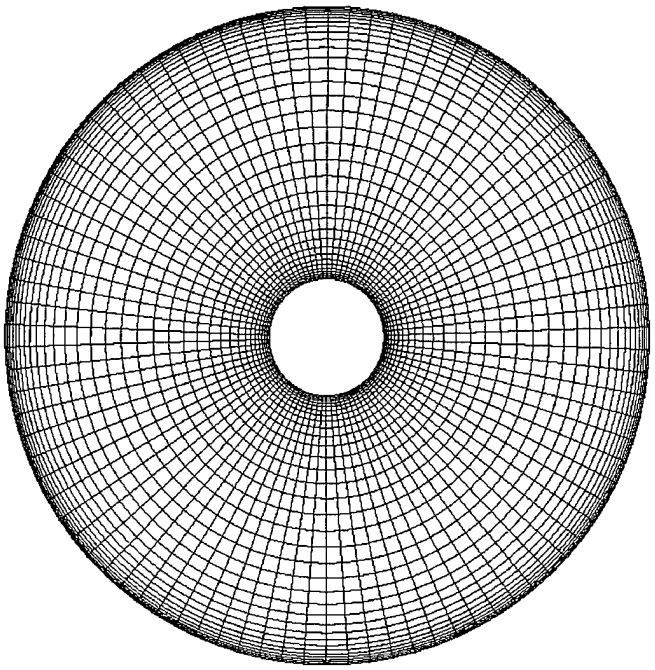

Figure 9. Computational mesh blanking for the (center tube) launcher.

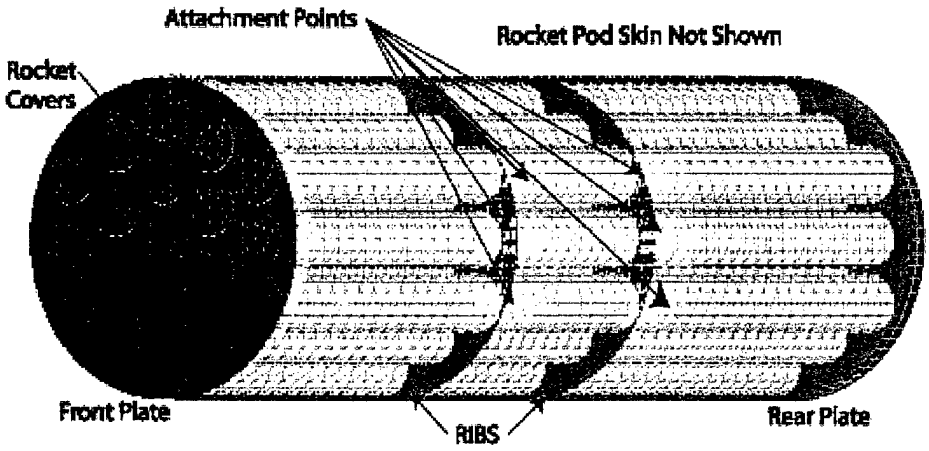

Figure 10. Initial rocket pod analysis with constraints set on the surface of the pod.

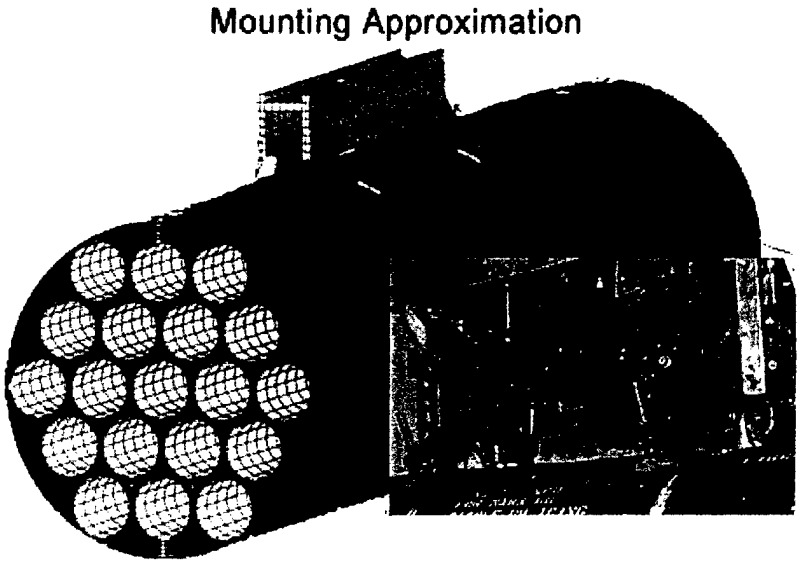

Figure 11. Mounting unit with the mounting bracket attached.

5. Results

5.1 CFD Results

Numerous CFD computations were performed using several different launch tube positions, with the rocket at various separation distances. The Mach numbers used were 0.15, 0.17, and 0.20, based on the distance between the rocket and the launcher. The computations were performed at 0° angle of attack, for atmospheric flight conditions. The CFD code ZNSFLOW [10] was used to perform the computations. All computations were performed on the SGI suite of supercomputers at the U.S. Army Research Laboratory (ARL) Major Shared Resource Center (MSRC). Resources required for the 2-D computations were minimal. For the 3-D calculations, each case required 6.5-million words of memory and, on average, 80 hr of computer time. The number of processors used ranged from 8 to 16, based on machine availability.

Two-dimensional axisymmetric steady-state calculations were first completed with the rocket positioned 20 in from the launcher at a Mach number of 0.15 and 0° angle of attack. For this case, the tube in the launcher was not modeled. Both stationary and moving boundary conditions along the launcher were considered. Figure 12 shows Mach contours for these two cases to be quite different. Computed pressures along the front surface of the launcher show that the highest pressure is found in the center of the launcher pod. The maximum pressure is slightly higher for the moving boundary conditions.

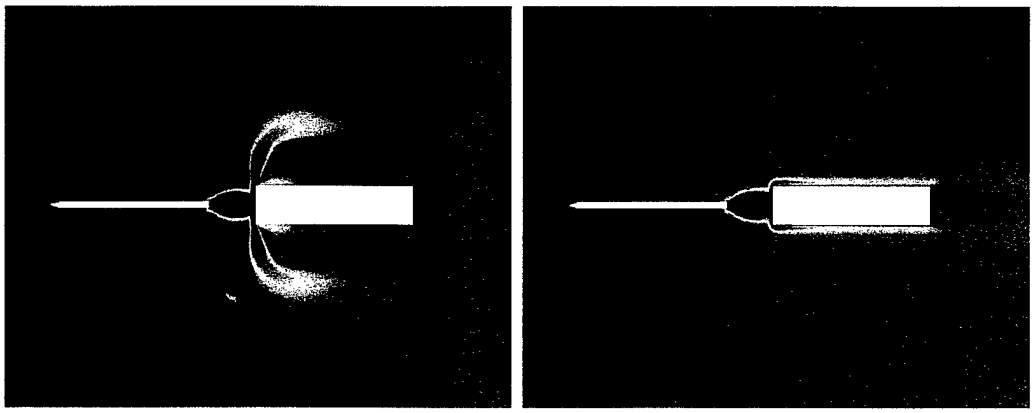

(a) (b)

Figure 12. Mach contours without tube, (a) pod moving and (b) stationary.

The next step in the process was to model the center tube and perform computations with the rocket at S = 20, S = 33, and S = 66 (see Figure 7). Again, 2-D axisymmetric calculations were carried out. Mach numbers used were 0.15, 0.17, and 0.20 for S = 20, S = 33, and S = 66, respectively, while the angle of attack was 0° for all cases. For comparison purposes, the calculations were performed with and without modeling the launch tube. The computed surface pressures on the front of the launcher are shown in Figures 13 and 14, respectively. Positions 1, 2, and 3 correspond to S =20, S = 33, and S = 66. For both models, the pressure near the center of the launcher decreases as distance between the rocket and launcher increases. The difference in maximum pressure also decreases as the separation distance increases (Figure 13). The surface pressures inside the tube show this same trend (Figure 14). Figure 15 shows qualitative pressure contours for the computations for the case where the launch tube was modeled.

Finally, the 3-D steady-state computations were undertaken. The center tube location at S = 20 was computed first and compared with the previous 2-D axisymmetric results. Figure 16 shows that the flow fields are quite similar. The surface pressure comparison shown in Figure 17 confirms this similarity. Data presented by Costello [18] supplied pitch and yaw for the rocket as it exited the center tube of the launcher. Consequently, calculations were performed for the center tube launch at S = 20, S = 33, and S = 66 with pitch and yaw. Figure 18 shows the difference in pressure inside the center tube for S = 20, based on the difference in pitch and yaw. Qualitative analysis of the surface pressure, as depicted in Figures 19, 20, and 21, show that high-pressure covers more of the forward surface of the launcher as the separation distance increases. Although the flow is symmetric at S = 20, it becomes slightly asymmetric as the separation distance increases, again due to the change in pitch and yaw.

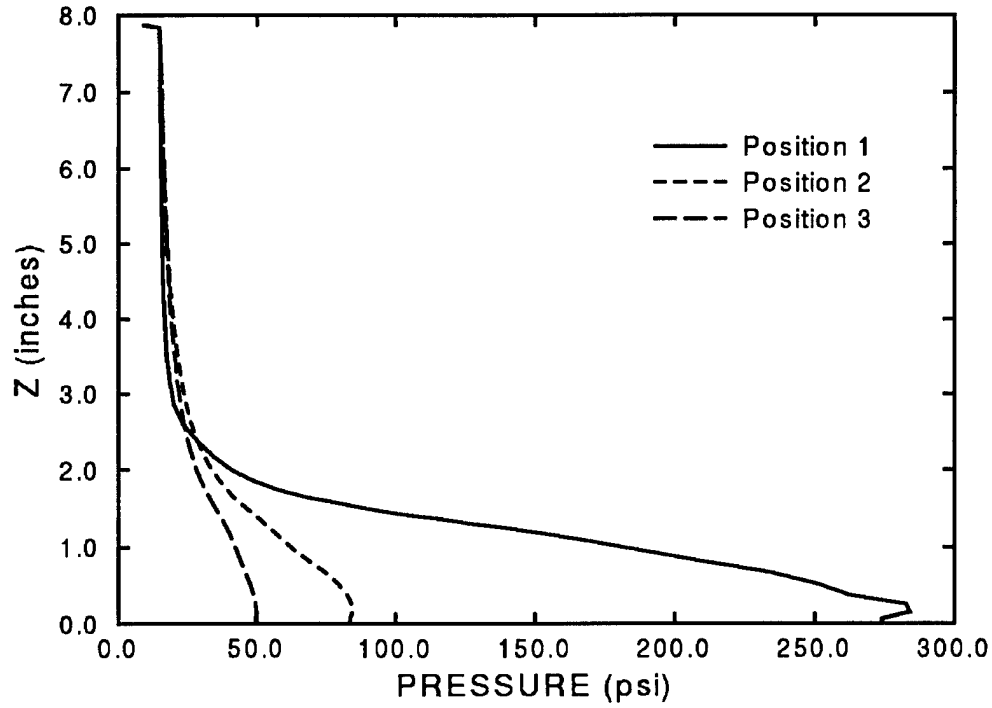

Figure 13. Pressure on launcher, model without tube.

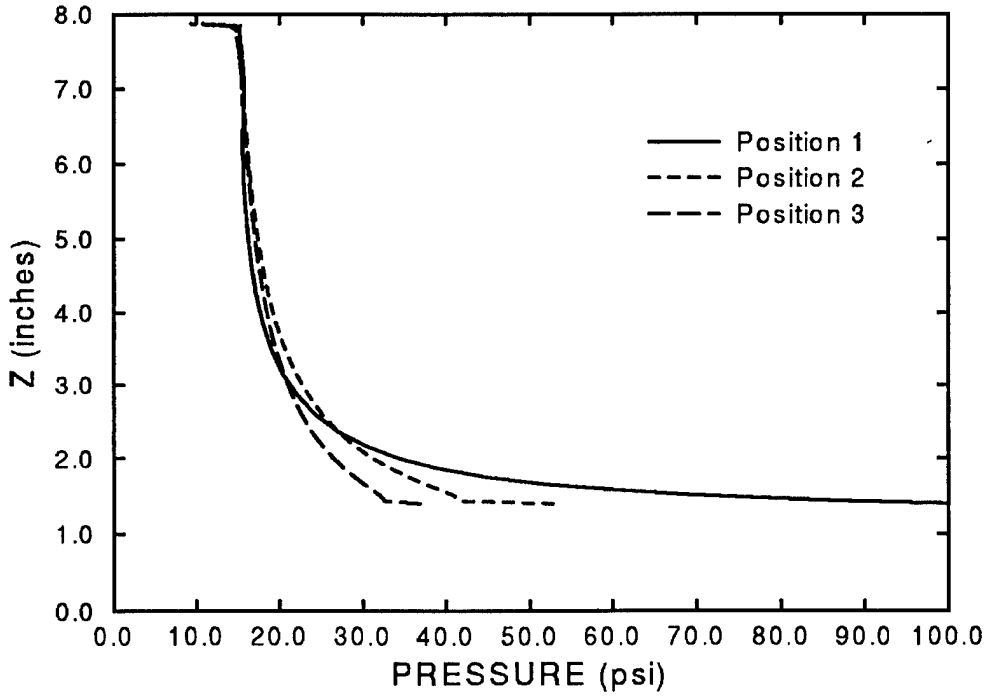

Figure 14. Pressure on launcher, model with tube.

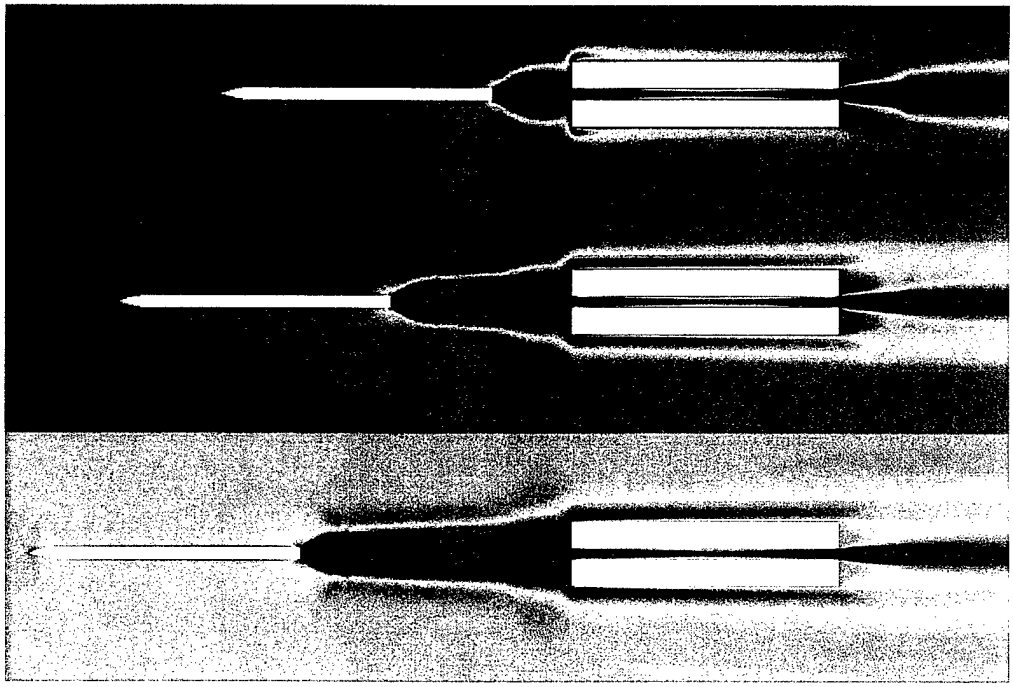

Figure 15. Pressure contours at various separation distances, model with tube.

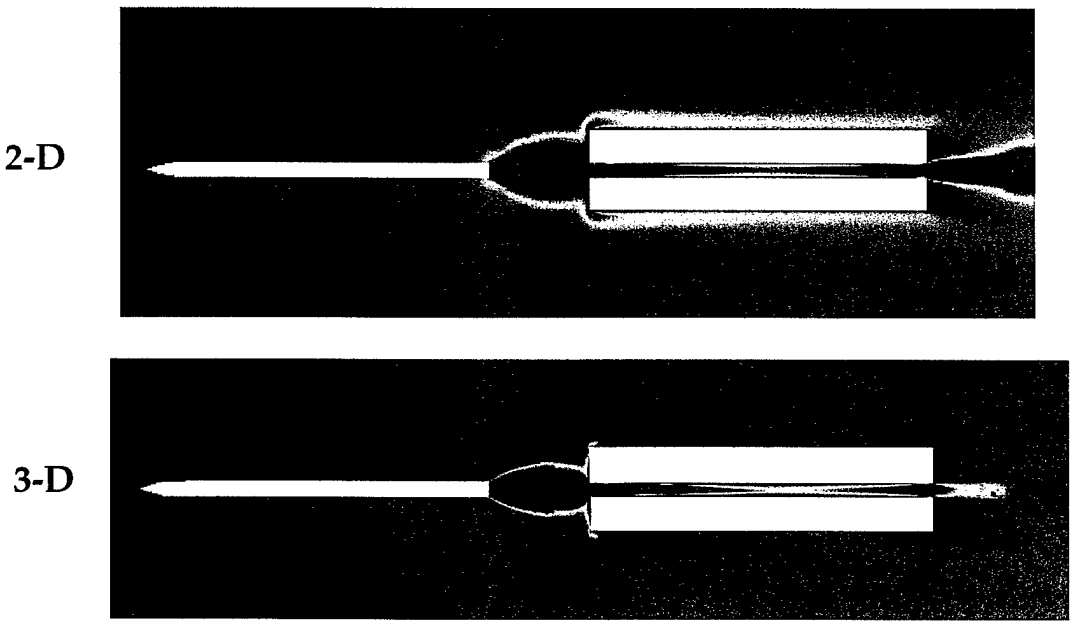

Figure 16. Comparison of 2-D and 3-D calculations.

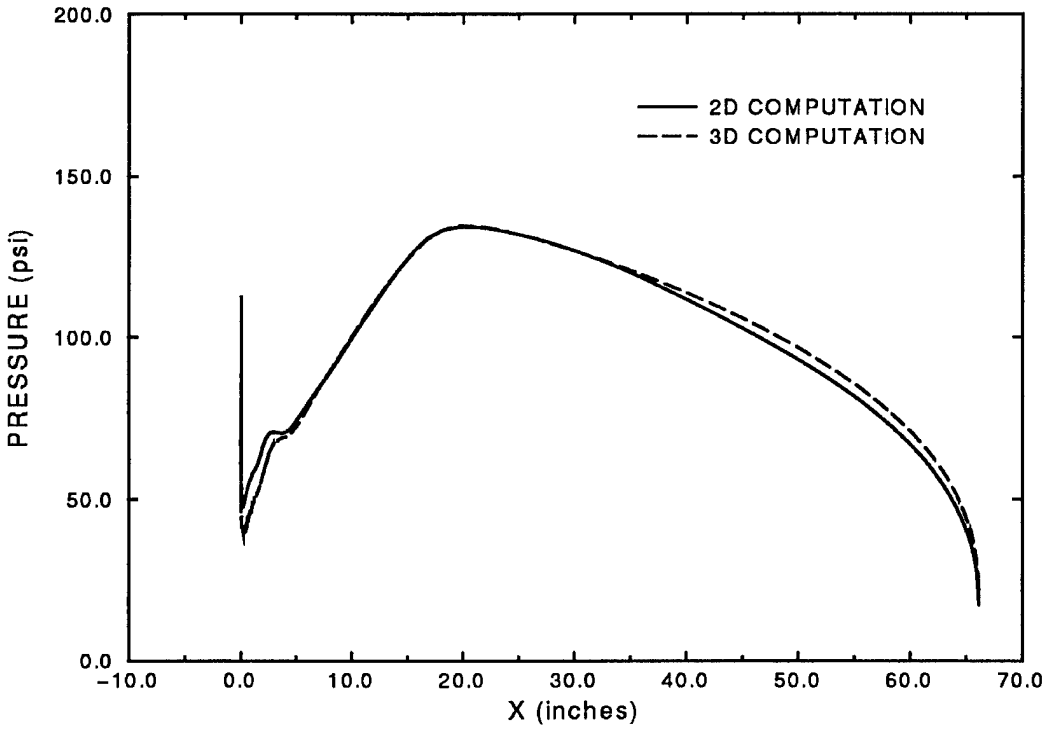

Figure 17. Surface pressure comparison, center tube, at S = 20.

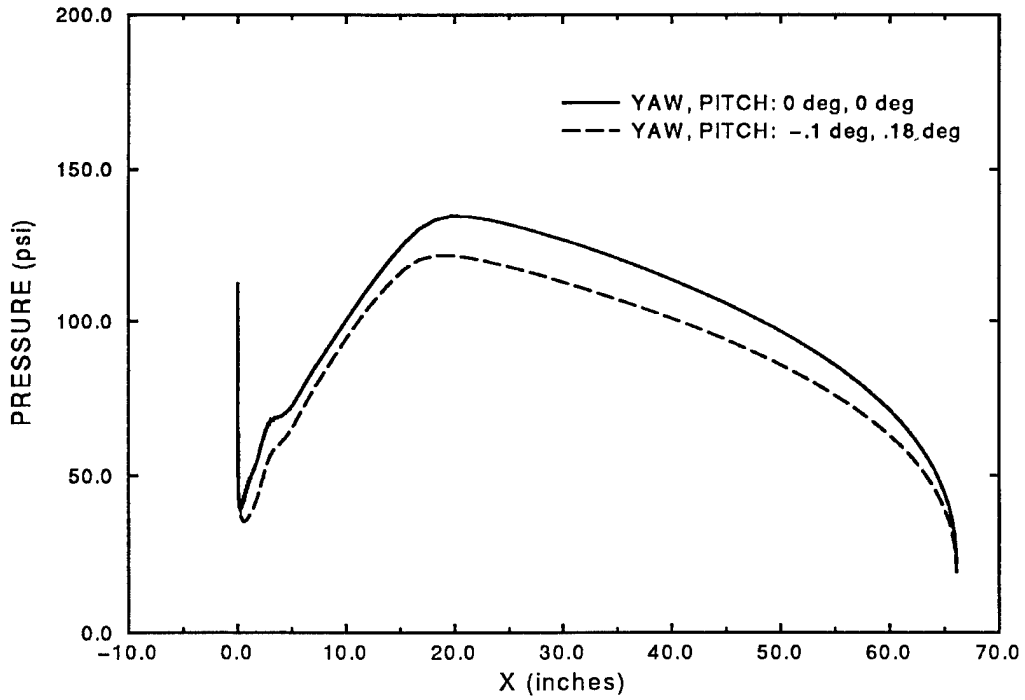

Figure 18. Comparison of pitch and yaw, center tube, at S = 20.

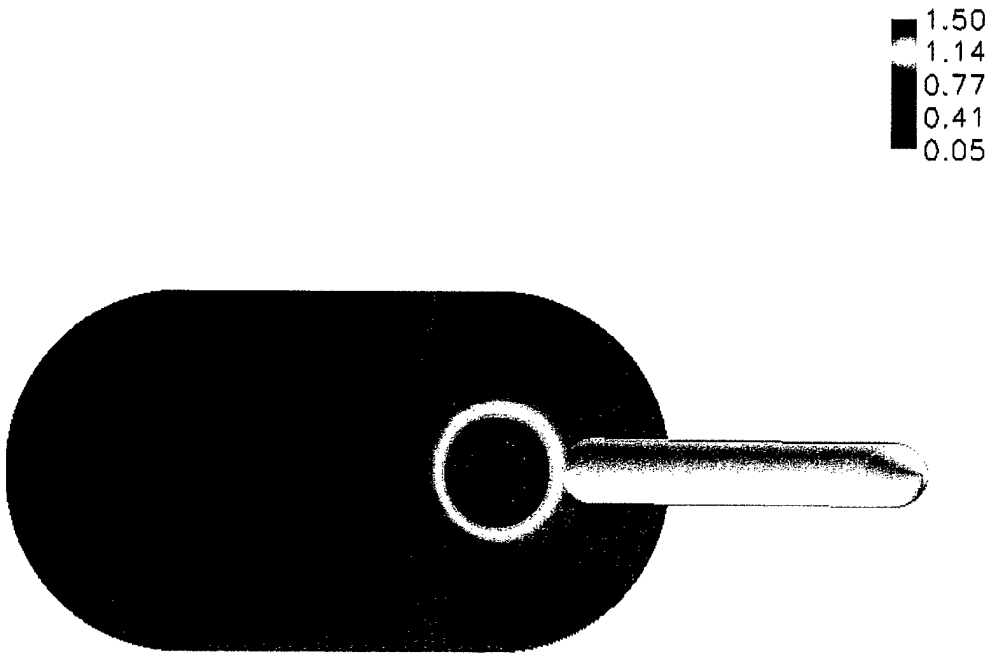

Figure 19. Surface pressure on launcher, center tube, at S = 20.

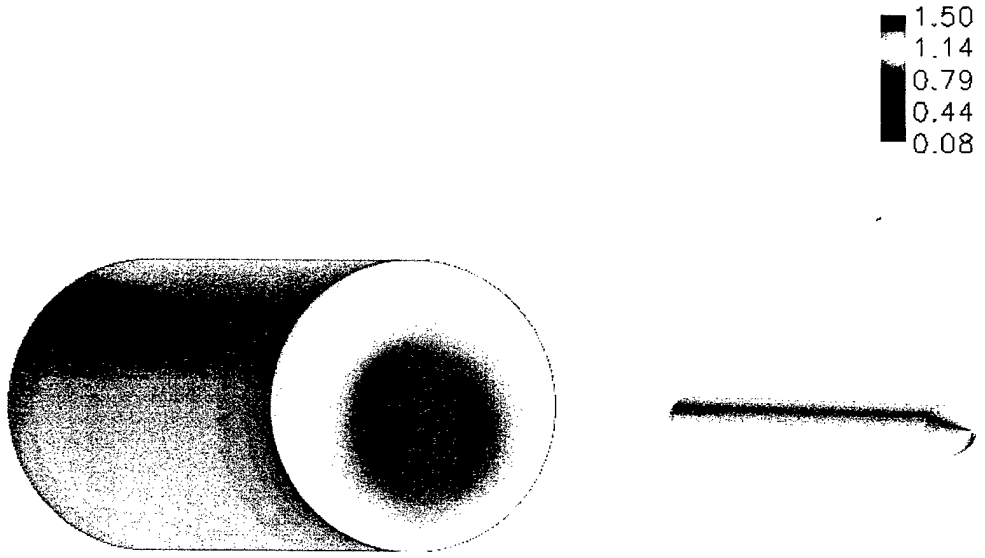

Figure 20. Surface pressure contours, center tube, at S = 33.

Computed results obtained for the asymmetric (or offset) launch tube locations are presented next. For these calculations, pitch and yaw are zero. Figure 22 shows surface pressure contours on the forward pod surface, for all three launch tube locations, at S = 20. This same view is presented in Figure 23 for S = 33. A

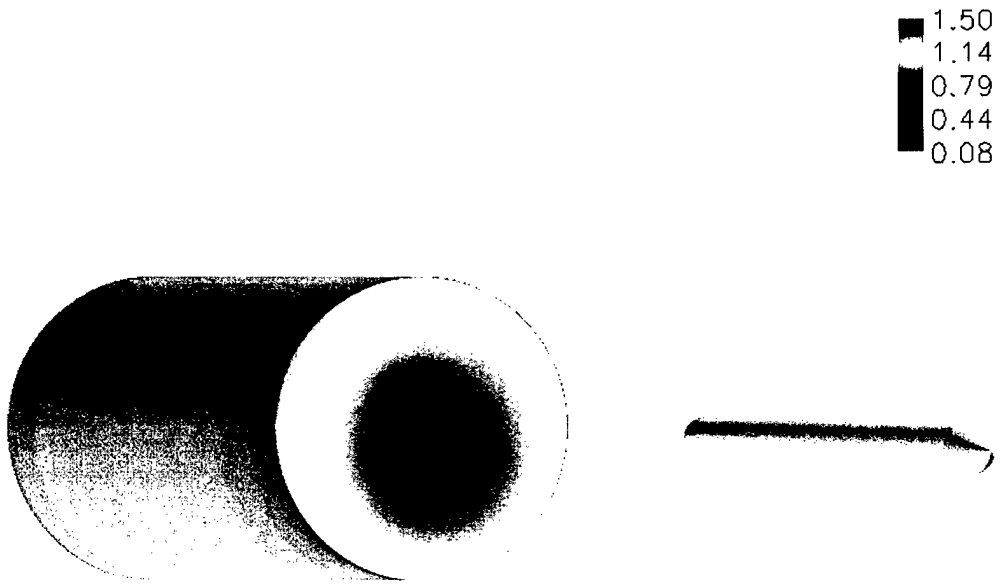

Figure 21. Surface pressure contours, center tube, at S = 66.

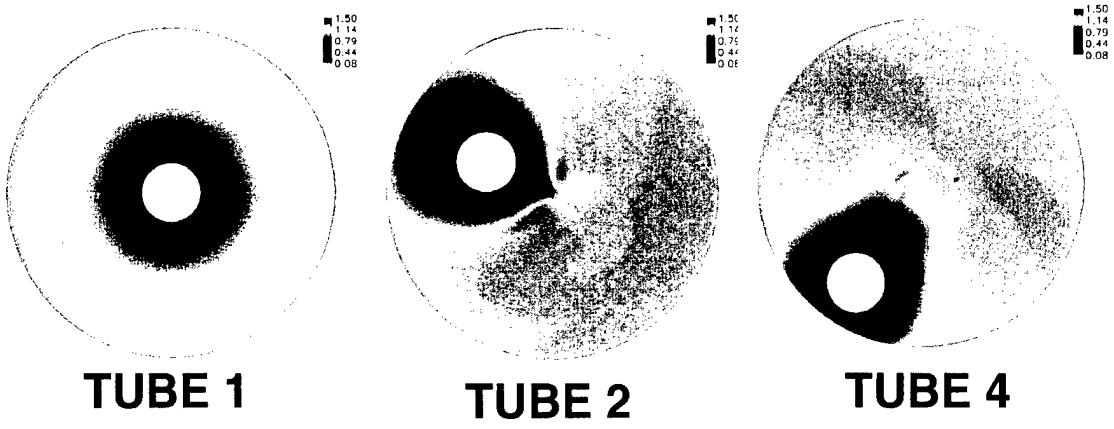

Figure 22. Pressure contours on forward pod surface, at S = 20.

longitudinal view of the pressure contours on the launch pod for each of the three tube positions is shown in Figure 24. As seen in these figures, the flow field on the front and side surfaces changes dramatically when the rocket is launched from the different tubes. When the rocket is launched from the center tube, the pressure contours are symmetric at S = 20. While there is a slight asymmetry on the forward surface at S = 33, the flow on the side of the launcher is unchanged.

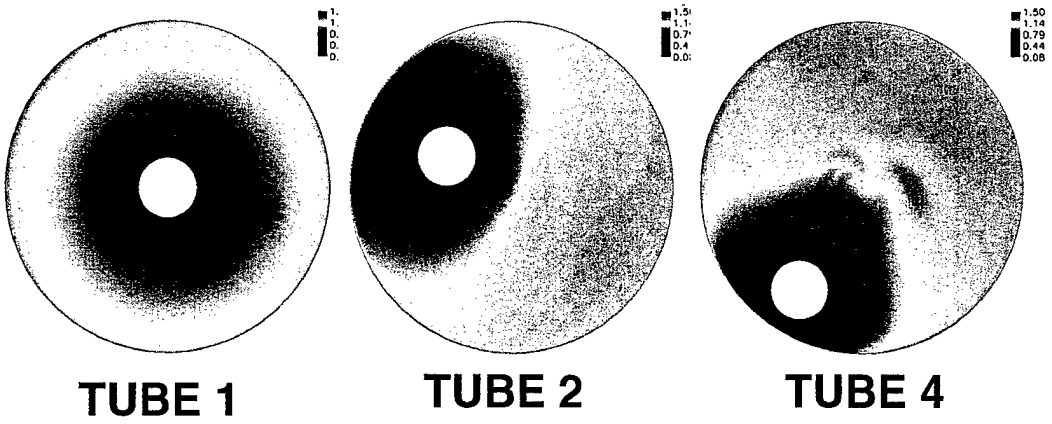

Figure 23. Pressure contours on forward pod surface, at S = 33.

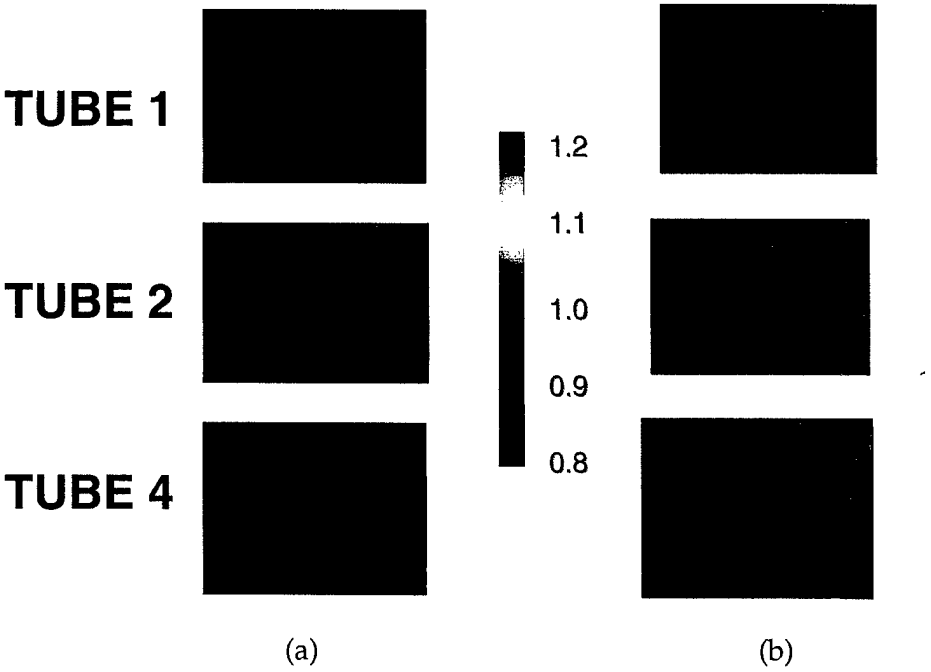

Figure 24. Pressure contours on side of pod, at (a) S = 20 and at (b) S = 33.

As expected, this is not so for the asymmetric tube locations, for all separation distances considered. The flow on both the forward and side surfaces of the launcher are affected. The asymmetrical aerodynamic loading for the offset tube cases can have a significant effect on the structural integrity of the rocket launcher. Coupling of the CFD results to SD analysis of the launcher is presented in the next section.

5.2 SD Results

As described earlier, CFD results provided the loading used in the SD calculations. Simulations were run for both FEM models, using the center tube as the launch tube. The pressures applied to the surface were done at three different rocket distances and are shown in Figures 25–27. Stresses for each case were compared and showed that the peak stress condition in the static calculation occurred just after the rocket exited the rocket pod. Calculations were performed with the center hole open and with it closed off by a thin membrane for comparison.

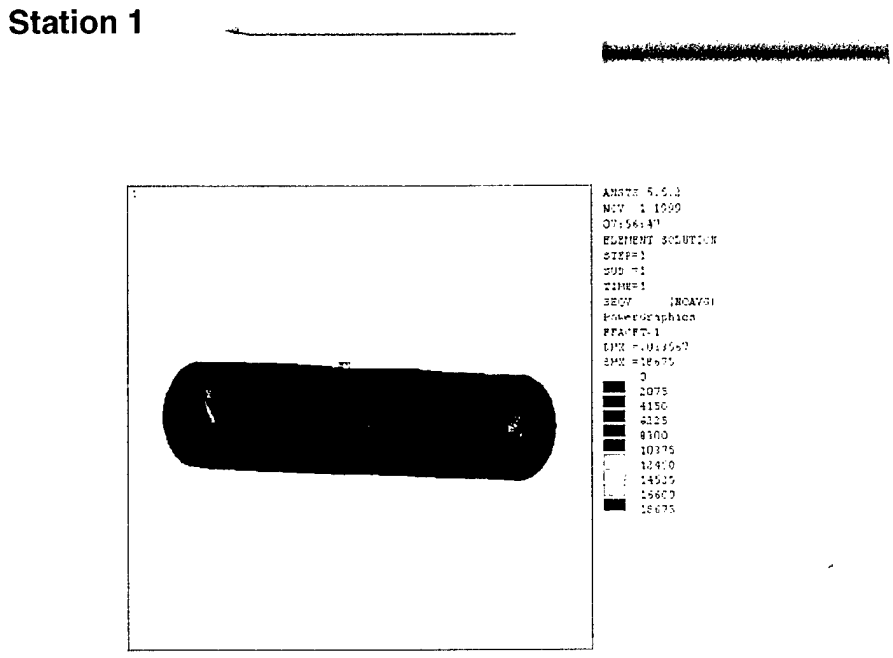

Figure 25. Von-Mises stress contours, center tube, at S = 20.

In Figures 26 and 27, Von-Mises stresses are used for comparison. The figures show exaggerated displacements and stresses. Static displacements and stresses would undoubtedly be smaller than those found in a dynamic calculation. The dynamic calculation or the coupling of the time dependent pressures will be the next phase in this study. The original constraints proved to be unrealistic. In laboratory tests, it was observed that the rocket pod exhibited considerable lateral movement, particularly with rocket pods fired off the centerline axis. However, the calculations for the first set of constraints showed pitching motion due mainly to pod flexure as the primary source of movement. By including a crude approximation for the mounting bracket and simulating rockets being launched from off axis tubes, the left right motion increased. To fine tune the boundary constraints, several controlled laboratory experiments of the pod in

Station 2

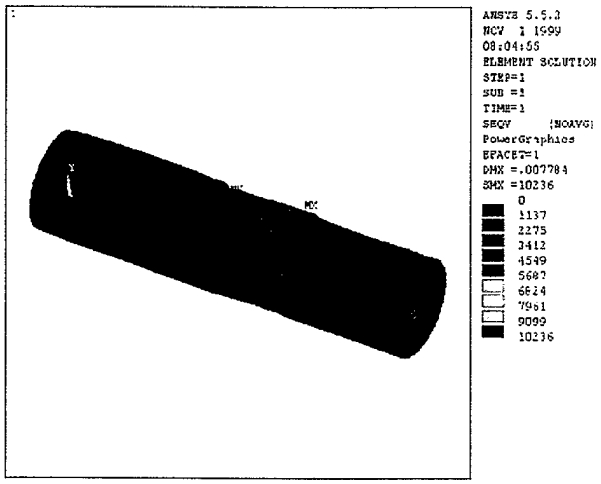

Figure 26. Von-Mises stress contours, center tube, at S = 33.

Station 3

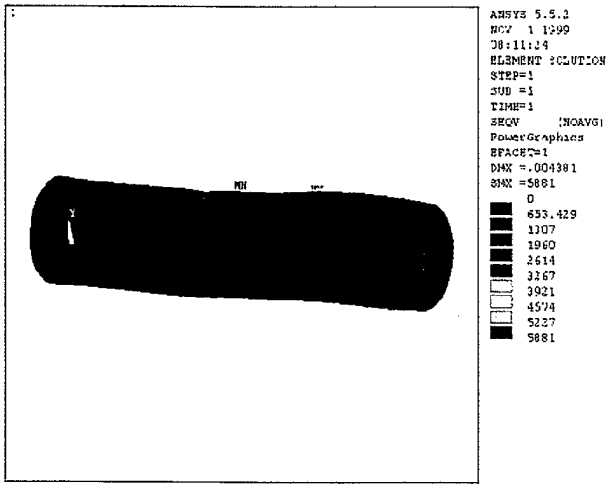

Figure 27. Von-Mises stress contours, center tube, at S = 66.

comparison to simulations would be needed. This was beyond the scope and time constraints of the demonstration. By working with CFD modelers, the problems and potential solutions to coupling CFD calculations were identified. A piecemeal approach to developing the interface was taken and calculation were successfully made.

6. Conclusion

A computational study was undertaken to investigate the aerodynamics of an MLRS consisting of an ogive-cylinder rocket and a cylindrical launch pod. Flow field computations have been performed at Mach numbers 0.15, 0.17 and 0.20, for 0° angle of attack, using a steady, zonal F3D Navier-Stokes code and the Chimera composite grid discretization technique. The computed CFD results for various rocket and tube positions produced surface pressure data that was used as input to finite element codes and to assist in the structural analysis of the system, particularly the location of high stress points. Several calculations were completed. These efforts have identified the need for additional generalization and fine tuning of the CFD/SD interface. This effort represents a first step towards achieving a multidisciplinary coupled CFD/SD method for applications of interest to the U.S. Army. Further work is needed to develop a strongly coupled CFD/SD method wherein SD provides feedback (a new shape) to CFD as well.

7. References

1. Sahu, J., and J. L. Steger. "Numerical Simulations of Transonic Flows." *International Journal for Numerical Methods in Fluids*, vol. 10, no. 8, pp. 855–873, 1990.

2. Ferry, E. N., J. Sahu, and K. R. Heavey. "Navier-Stokes Computations of Sabot Discard Using Chimera Scheme." Proceedings of the 16th International Symposium on Ballistics, San Francisco, CA, September 1996.

3. Sahu, J., K. R. Heavey, and E. N. Ferry. "Computational Fluid Dynamics for Multiple Projectile Configurations." Proceedings of the Third Overset Composite Grid and Solution Technology Symposium, Los Alamos, NM, October 1996.

4. Sahu, J., and C. J. Nietubicz. "Application of Chimera Technique to Projectiles in Relative Motion." ARL-TR-590, U.S. Army Research Laboratory, Aberdeen Proving Ground, MD, October 1994.

5. Sahu, J., K. R. Heavey, and C. J. Nietubicz. "Time-Dependent Navier-Stokes Computations for Submunitions in Relative Motion." Proceedings of the Sixth International Symposium on Computational Fluid Dynamics, Lake Tahoe, NV, September 1995.

6. Sahu, J., H. L. Edge, K. R. Heavey, and E. N. Ferry. "Computational Fluid Dynamics Modeling of Multi-Body Missile Aerodynamic Interference." ARL-TR-1765, U.S. Army Research Laboratory, Aberdeen Proving Ground, MD, August 1998.

7. Steger, J. L., F. C. Dougherty, and J. A. Benek. "A Chimera Grid Scheme." *Advances in Grid Generation*, FED-5, edited by K. N. Ghia and U. Ghia, American Society of Mechanical Engineers, June 1983.

8. Benek, J. A., T. L. Donegan, and N. E. Suhs. "Extended Chimera Grid Embedding Scheme With Application to Viscous Flows." American Institute of Aeronautics and Astronautics Paper No. 87–1126-CP, 8th AIAA Computational Fluids Dynamics Conference, Honolulu, HI, 1987.

9. Buning, P. G., I. T. Chiu, S. Obayashi, Y. M. Rizk, and J. L. Steger. "Numerical Simulation of the Integrated Space Shuttle Vehicle in Ascent." American Institute of Aeronautics and Astronautics Atmospheric Flight Mechanics Conference, Minneapolis, MN, August 1988.

10. Edge, H. L., J. Sahu, W. B. Sturek, D. M. Pressel, K. R. Heavey, P. Weinacht, C. K. Zoltani, C. J. Nietubicz, J. Clarke, M. Behr, and P. Collins. "Common High Performance Computing Software Support Initiative (CHSSI)

Computational Fluid Dynamics CFD-6 Project Final Report: ARL Block-Structured Gridding Zonal Navier-Stokes Flow (ZNSFLOW) Solver Software." ARL-TR-2084, U.S. Army Research Laboratory, Aberdeen Proving Ground, MD, February 2000.

11. Pulliam, T. H., and J. L. Steger. "On Implicit Finite-Difference Simulations of Three-Dimensional Flow." *American Institute of Aeronautics and Astronautics*, vol. 18, no. 2, pp. 159–167, February 1982.

12. Baldwin, B. L., and H. Lomax. "Thin Layer Approximation and Algebraic Model for Separated Turbulent Flows." AIAA Paper 78-257, American Institute of Aeronautics and Astronautics, Reston, VA, January 1978.

13. Goldberg, U. C., O. Peroomian, and S. Chakravarthy. "A Wall-Distance Free K-E Model With Enhanced Near-Wall Treatment." *American Society of Mechanical Engineers Journal of Fluids Engineering*, vol. 120, pp. 457–462, 1998.

14. Suhs, N. E., and R. W. Tramel. "PEGSUS 4.0 User's Manual." AEDC-TR-8, Arnold Engineering Development Center, Arnold Air Force Base, TN, November 1991.

15. Wilkerson, S. A. "Bubble Jet Calculations Using the DYSMAS/E Finite Difference Code." NSWC TR 88-226, Naval Surface Weapons Command, Silver Spring, MD, 1988.

16. Wilkerson, S. A. "Ship and Submarine Response to an Underwater Explosion." Master's thesis, George Washington University, Washington, DC, May 1985.

17. Chan, W. M. OVERGRID Software Documentation. U.S. Army Research Laboratory-Major Shared Resource Center (ARL-MSRC), Aberdeen Proving Ground, MD, April 1999.

18. Costello, M. F. Personal communication with J. Sahu. Oregon State University, Corvallis, OR, July 2000.

NO. OF COPIES	ORGANIZATION
2	DEFENSE TECHNICAL INFORMATION CENTER DTIC OCA 8725 JOHN J KINGMAN RD STE 0944 FT BELVOIR VA 22060-6218
1	HQDA DAMO FDT 400 ARMY PENTAGON WASHINGTON DC 20310-0460
1	OSD OUSD(A&T)/ODDR&E(R) DR R J TREW 3800 DEFENSE PENTAGON WASHINGTON DC 20301-3800
1	COMMANDING GENERAL US ARMY MATERIEL CMD AMCRDA TF 5001 EISENHOWER AVE ALEXANDRIA VA 22333-0001
1	INST FOR ADVNCD TCHNLGY THE UNIV OF TEXAS AT AUSTIN 3925 W BRAKER LN STE 400 AUSTIN TX 78759-5316
1	US MILITARY ACADEMY MATH SCI CTR EXCELLENCE MADN MATH MAJ HUBER THAYER HALL WEST POINT NY 10996-1786
1	DIRECTOR US ARMY RESEARCH LAB AMSRL D DR D SMITH 2800 POWDER MILL RD ADELPHI MD 20783-1197

NO. OF COPIES	ORGANIZATION
1	DIRECTOR US ARMY RESEARCH LAB AMSRL CI AI R 2800 POWDER MILL RD ADELPHI MD 20783-1197
3	DIRECTOR US ARMY RESEARCH LAB AMSRL CI LL 2800 POWDER MILL RD ADELPHI MD 20783-1197
3	DIRECTOR US ARMY RESEARCH LAB AMSRL CI IS T 2800 POWDER MILL RD ADELPHI MD 20783-1197
	ABERDEEN PROVING GROUND
2	DIR USARL AMSRL CI LP (BLDG 305)

NO. OF COPIES	ORGANIZATION
2	USAF WRIGHT AERONAUTICAL LABORATORIES AFWAL FIMG DR J SHANG N E SCAGGS WPAFB OH 45433-6553
1	COMMANDER NAVAL SURFACE WARFARE CTR CODE B40 DR W YANTA DAHLGREN VA 22448-5100
1	COMMANDER NAVAL SURFACE WARFARE CTR CODE 420 DR A WARDLAW INDIAN HEAD MD 20640-5035
4	DIRECTOR NASA LANGLEY RESEARCH CTR D M BUSHNELL DR M J HEMSCH DR J SOUTH TECH LIB LANGLEY STATION HAMPTON VA 23665
2	DARPA DR P KEMMEY DR J RICHARDSON 3701 N FAIRFAX DR ARLINGTON VA 22203-1714
5	DIRECTOR NASA AMES RESEARCH CTR L SCHIFF MS 227 8 T HOLST MS 258 1 D CHAUSSEE MS 258 1 M RAI MS 258 1 B MEAKIN MS 258 1 MOFFETT FIELD CA 94035
3	AIR FORCE ARMAMENT LAB AFATL FXA S C KORN B SIMPSON D BELK EGLIN AFB FL 32542-5434

NO. OF COPIES	ORGANIZATION
4	COMMANDER US ARMY TACOM ARDEC AMSTA AR FSF T C NG H HUDGINS J GRAU W KOENIG PICATINNY ARSENAL NJ 07806-5000
1	COMMANDER US ARMY TACOM AMSTA AR CCH B P VALENTI BLDG 65 S PICATINNY ARSENAL NJ 07806-5001
1	COMMANDER US ARMY ARDEC SFAE FAS SD M DEVINE PICATINNY ARSENAL NJ 07806-5001
1	COMMANDER US NAVAL SURFACE WPNS CTR DR F MOORE DAHLGREN VA 22448
2	UNIV OF CALIFORNIA DAVIS DEPT OF MECHANICAL ENG H A DWYER M HAFEZ DAVIS CA 95616
1	AEROJET ELECTRONICS PLANT D W PILLASCH B170 DEPT 5311 PO BOX 296 1100 WEST HOLLYVALE ST AZUSA CA 91702
1	MIT TECH LIBRARY 77 MASSACHUSETTS AVE CAMBRIDGE MA 02139

NO. OF
COPIES ORGANIZATION

1 DIRECTOR
LANL
B HOGAN
MS G770
LOS ALAMOS NM 87545

3 DIRECTOR
SANDIA NATIONAL LABS
DR W OBERKAMPF DIV 1554
DR F BLOTTNER DIV 1554
DR W WOLFE DIV 1636
ALBUQUERQUE NM 87185

1 NAVAL AIR WARFARE CENTER
D FINDLAY
MS3 BLDG 2187
PATUXENT RIVER MD 20670

1 METACOMP TECHNOLOGIES INC
S R CHAKRAVARTHY
650 HAMPSHIRE RD STE 200
WESTLAKE VILLAGE CA
91361-2510

3 COMMANDER
USAAMCOM
AMSAM RD SS AS
E KREEGER
C D MIKKELSON
E VAUGHN
REDSTONE ARSENAL AL
35898-5252

1 COMMANDER
US ARMY TACOM ARDEC
AMCPM DS MO
P J BURKE
BLDG 162S
PICATINNY ARSENAL NJ
07806-5000

1 COMMANDER
USAAMCOM
AMSAM RD SS
G LANDINGHAM
REDSTONE ARSENAL NJ
35898-5252

1 ADVANCED TECHNOLOGY CTR
ARVIN CALSPAN
AERODYNAMICS RSCH DEPT
DR M S HOLDEN
PO BOX 400
BUFFALO NY 14225

1 UIUC
DEPT OF MECHANICAL AND
INDUSTRIAL ENGINEERING
DR J C DUTTON
URBANA IL 61801

1 UNIVERSITY OF MARYLAND
DEPT OF AEROSPACE ENG
DR J D ANDERSON JR
COLLEGE PARK MD 20742

1 UNIVERSITY OF TEXAS
DEPT OF AEROSPACE ENG
MECHANICS
DR D S DOLLING
AUSTIN TX 78712-1055

ABERDEEN PROVING GROUND

3 CDR
US ARMY ARDEC
FIRING TABLES BR
R LIESKE
R EITMILLER
F MIRABELLE
BLDG 120
APG MD 21005

25 DIR USARL
AMSRL CI H
C NIETUBICZ
AMSRL CI HC
J BENEK
R NOACK
S WILKERSON
AMSRL SL BE
A MIKHAIL
AMSRL WM
J SMITH
AMSRL WM B
A W HORST JR
W CIEPIELA

NO. OF COPIES	ORGANIZATION
	AMSRL WM BA
	D LYON
	T BROWN
	AMSRL WM BC
	P PLOSTINS
	J DESPIRITO
	B GUIDOS
	K HEAVEY
	J SAHU (5 CPS)
	S SILTON
	P WEINACHT
	AMSRL WM BD
	B FORCH
	M NUSCA
	AMSRL WM BF
	J LACETERA
	H EDGE

REPORT DOCUMENTATION PAGE

Form Approved
OMB No. 0704-0188

1. AGENCY USE ONLY *(Leave blank)*	2. REPORT DATE	3. REPORT TYPE AND DATES COVERED
	April 2002	Final, October 1999–October 2000

4. TITLE AND SUBTITLE
A Multidisciplinary Coupled Computational Fluid Dynamics (CFD) and Structural Dynamics (SD) Analysis of a 2.75-in Rocket Launcher

5. FUNDING NUMBERS
1L162618AH80

6. AUTHOR(S)
Karen R. Heavey, Jubaraj Sahu, and Stephen A. Wilkerson

7. PERFORMING ORGANIZATION NAME(S) AND ADDRESS(ES)
U.S. Army Research Laboratory
ATTN: AMSRL-WM-BC
Aberdeen Proving Ground, MD 21005-5066

8. PERFORMING ORGANIZATION REPORT NUMBER
ARL-MR-529

9. SPONSORING/MONITORING AGENCY NAMES(S) AND ADDRESS(ES)

10.SPONSORING/MONITORING AGENCY REPORT NUMBER

11. SUPPLEMENTARY NOTES

12a. DISTRIBUTION/AVAILABILITY STATEMENT
Approved for public release; distribution is unlimited.

12b. DISTRIBUTION CODE

13. ABSTRACT ***(Maximum 200 words)***

A multidisciplinary effort was undertaken to investigate the effect of aerodynamic loading on the structural integrity of a multiple launch rocket system of interest to the U.S. Army. Computational fluid dynamics (CFD) techniques have been used to obtain numerical solutions for the flow field of a rocket and launcher. Computed results have been obtained for several launch tubes, with the rocket at separation distances of 20, 33, and 66 in. Qualitative flow field features show the surface pressure on the surface of both the projectile and the launcher. The surface pressure data on the launcher was then extracted from the solution files. Software was developed to couple this data to a structural dynamics (SD) solver. CFD results provided the aerodynamic loading component used during the initial portion of the launch sequence. The SD code was subsequently used to calculate stress points on the launcher. These results represent a first step in an effort to generalize and fine tune the CFD/SD interface.

14. SUBJECT TERMS
multidisciplinary, computational fluid dynamics, structural dynamics, pressure loading, multiple launch rocket system, aerodynamic

15. NUMBER OF PAGES
35

16. PRICE CODE

17. SECURITY CLASSIFICATION OF REPORT	18. SECURITY CLASSIFICATION OF THIS PAGE	19. SECURITY CLASSIFICATION OF ABSTRACT	20. LIMITATION OF ABSTRACT
UNCLASSIFIED	UNCLASSIFIED	UNCLASSIFIED	UL

INTENTIONALLY LEFT BLANK.